

# Experimental demonstration of frequency downconverted arm length stabilization for a future upgraded gravitational wave detector

SATOSHI TANIOKA<sup>1,\*</sup>, BIN WU<sup>1</sup>, AND STEFAN W. BALLMER<sup>1</sup>

<sup>1</sup>Department of Physics, Syracuse University, Syracuse, New York 13244, USA

\*stanioka@syr.edu

Compiled May 3, 2024

Ground-based laser interferometric gravitational wave detectors consist of complex multiple optical cavity systems. An arm-length stabilization (ALS) system has played an important role in bringing such complex detector into operational state and enhance the duty cycle. The sensitivity of these detectors can be improved if the thermal noise of their test mass mirror coatings is reduced. Crystalline AlGaAs coatings are a promising candidate for this. However, traditional ALS system with frequency-doubled 532 nm light is no longer an option with AlGaAs coatings due to the narrow bandgap of GaAs, thus alternative locking schemes must be developed. In this letter, we describe an experimental demonstration of a novel ALS scheme which is compatible with AlGaAs coatings. This ALS scheme will enable the use of AlGaAs coatings and contribute to improved sensitivity of future detectors.

<http://dx.doi.org/10.1364/ao.XX.XXXXXX>

Ground-based gravitational wave detectors (GWDs) have opened a new window to the Universe by enabling direct detection of gravitational waves (GWs) [1–3]. Those GWDs are based on a Michelson interferometer with multiple optical cavities, and one needs to control lengths of 5 degrees of freedom (DoFs) in order to operate the detectors [4]. Their sensing signals are interdependent as the cavities are coupled with each other. An arm length stabilization (ALS) system is indispensable to robustly bring such an interferometer to the operating state [5–8]. Current terrestrial GWDs, such as Advanced LIGO, employ 532 nm wavelength green lasers generated via second harmonic generation (SHG) as an auxiliary laser for the ALS system. This enables us to pre-stabilize the arm cavity lengths independently from other DoFs.

The sensitivity of current GWD is partially limited by coating thermal noise [9, 10]. In order to enhance the GW detection rate, and hence their scientific impact, further upgrades are planned

to improve the sensitivity by introducing lower thermal noise coatings and better squeezing [11]. Crystalline gallium arsenide (GaAs) and aluminum-alloyed gallium arsenide ( $\text{Al}_x\text{Ga}_{1-x}\text{As}$ ) coatings (referred to as AlGaAs coatings) are a promising coating candidate for future GWDs, resulting in a factor of at least about 5 improvement in coating thermal noise compared to that of current Advanced LIGO [9, 12].

While crystalline AlGaAs coatings can largely reduce thermal noise, they are opaque to the auxiliary 532 nm laser light due to the narrow bandgap of GaAs [13]. Therefore, a new ALS scheme will need to be defined in order to implement AlGaAs coated mirrors. To solve this problem, a novel ALS scheme was proposed by the author (ST) in which the frequency downconverted 2128 nm laser by an optical parametric oscillation (OPO) can be used instead of traditional 532 nm green laser [12].

In this letter, we describe the experimental demonstration of the novel ALS scheme using frequency downconverted light. We developed a tabletop proof-of-concept setup to demonstrate the frequency downconverted ALS, and evaluated its performance. This setup is using amorphous coatings, but it is compatible with AlGaAs coatings. In addition, we propose a possible ALS scheme which can be applied to a cryogenic GWD by utilizing the demonstrated ALS scheme.

**Table 1. Main dichroic cavity parameters.**

| Parameter                  | Value   |
|----------------------------|---------|
| Cavity length              | 40 cm   |
| Free spectral range        | 375 MHz |
| Finesse for 1064 nm        | ~ 250   |
| FWHM linewidth for 1064 nm | 2.2 nm  |
| Finesse for 2128 nm        | ~ 30    |

Fig. 1 shows the schematic of experimental setup for wavelength doubling ALS demonstration. Both the main and auxiliary 1064 nm laser sources are NPRO lasers made by Coherent. The beat note is detected by an RF photodiode (RFPD) to measure the frequency difference between the main and the auxiliary lasers. The delay line frequency discriminator (DFD) is used in

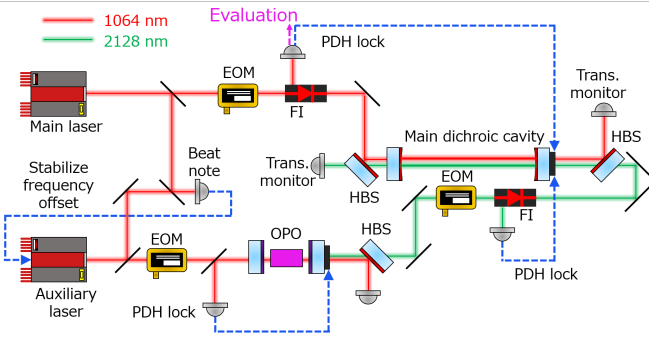


**Fig. 1.** Schematic of the ALS demonstration setup. Solid lines are optical paths, and dashed lines are electronics. Two free-running NPRO lasers are used as the main or auxiliary lasers. The main and the auxiliary beams are combined or separated by using a harmonic beam separator (HBS). Reflected beams from the main cavity are picked off by Faraday isolators (FIs). The main cavity is composed of a pair of amorphous coated mirrors. To imitate the input test mass of Advanced LIGO, these mirrors were designed to have reflectivities of 98.6% and about 96% at 1064 nm and 2128 nm, respectively [7]. This setup was installed on an optical table with pneumatic vibration isolators to mitigate seismic vibration coupling.

our setup in the same manner as previous work [6]. The noise of the delay line is estimated at about  $1 \text{ Hz}/\sqrt{\text{Hz}}$ . The DFD signal is sent to the auxiliary laser piezo transducer (PZT) so that the frequency offset was stabilized. This configuration enables us to keep the main laser off-resonant condition and bring it to a resonant point by changing the frequency offset as mentioned below.

One of the lasers is locked to the OPO cavity by PDH method to generate downconverted 2128 nm light [14, 15]. The OPO cavity is composed by a Fabry-Pérot cavity and a periodically poled potassium titanyl phosphate (PPKTP) crystal made by Raicol. Pound-Drever-Hall (PDH) locking of the OPO cavity is achieved by actuating the cavity length using a PZT attached on the output mirror.

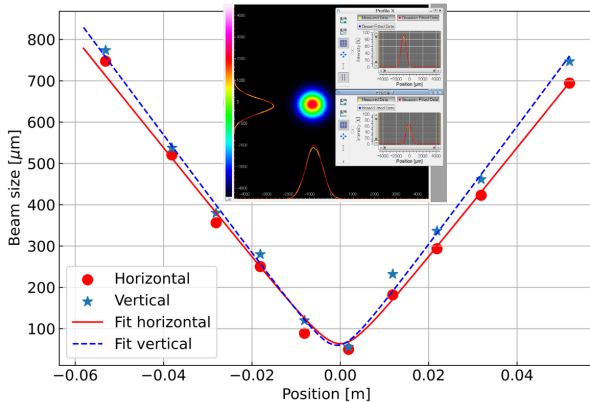


**Fig. 2.** Beam profile of the auxiliary laser and screenshot of the beam profiler application. Red circle and blue star are beam radii of horizontal and vertical directions, respectively. Red solid and blue dashed lines are fitted curves.

The beam profile of the downconverted 2128 nm auxiliary

light was measured by BP209-IR2, a scanning-slit beam profiler by Thorlabs. Fig. 2 shows the measured beam profile, which maintains the Gaussian beam shape of the 1064 nm pump light. Also, its  $M^2$  factor is estimated to be about 1.1. Therefore, the auxiliary beam generated by the degenerate OPO has adequate beam quality to be implemented in a GWD as an auxiliary beam source.

The downconverted auxiliary beam is phase modulated by an electro-optic modulator (EOM) for PDH locking to the main dichroic cavity. In our setup, the downconverted auxiliary laser is injected from the output side of the main cavity in the same manner as the previous works [5, 6]. The input beam powers are 6.5 mW and 2.5 mW for 1064 nm and 2128 nm beams, respectively. At the input or output port of the cavity, the main and the auxiliary beams are combined or separate by using a harmonic beam separator (HBS). The auxiliary PDH control signal is fed back to the cavity length through a PZT on the output mirror. PDH locking for the main laser is also enabled by actuating the PZT. The transmitted main and auxiliary laser powers are monitored by a silicon PD and an extended InGaAs PD, respectively. The main cavity has finesse of  $\sim 250$  for the 1064 nm main laser and  $\sim 30$  for the downconverted 2128 nm laser. The parameters of the main cavity are listed on Table 1.

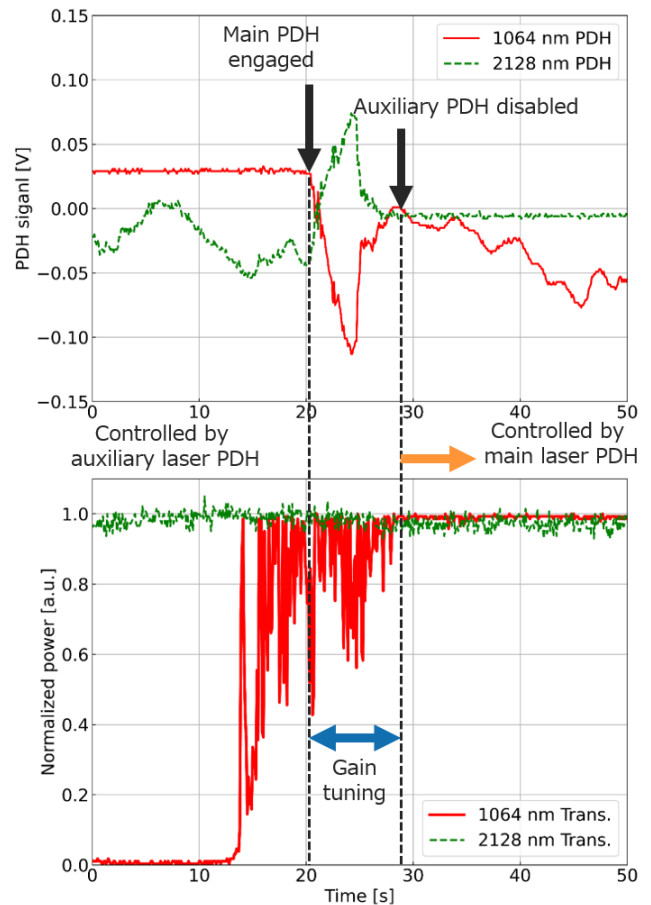


**Fig. 3.** Handing over the cavity length control from the auxiliary PDH to the main PDH. Top figure shows the PDH control signals of the main (solid red line) and auxiliary (dashed green line) lasers which are used to suppress disturbances. Bottom figure is the normalized transmitted powers of the main (solid red line) and auxiliary (dashed green line) lasers.

With this setup, we demonstrated the handover from the auxiliary laser to the main laser, hence the ALS with downconverted beam. We monitored the main and auxiliary PDH control signals and transmitted beam powers by a Tektronix MDO34 4-channel oscilloscope. Fig. 3 shows the time series data of handing over our ALS system. The cavity length was initially stabilized by the auxiliary laser PDH signal. On the other hand, the main laser was kept off resonance because the two NPRO lasers had a frequency offset controlled by the DFD. By adjusting the frequency offset, the main laser was brought to the resonant condition. Once it reached resonance, the frequency offset tuning was stopped and the main PDH control gain was increased so that its control was engaged. At the same time, the auxiliary PDH control gain was reduced to hand over the cavity length control to the main laser. After fine tuning the main PDH gain, the auxiliary PDH control was disabled and the cavity was controlled by the main laser PDH. As shown in Fig. 3, this process was successfully achieved without losing the cavity lock, i.e., the lock acquisition was achieved with 2128 nm downconverted auxiliary laser.

In addition to the demonstration of lock acquisition, we evaluated the performance of the ALS system. Here the goal was set for the displacement of the cavity in root mean square (RMS) to be below than the full width half-maximum (FWHM) linewidth in the same manner as the previous works [5, 6]. The FWHM linewidth can be given by

$$L_{\text{FWHM}} = \frac{\lambda}{2\mathcal{F}} \text{ [m]}, \quad (1)$$

where  $\lambda$  is the laser wavelength and  $\mathcal{F}$  is the cavity finesse. From Eq. (1), the FWHM cavity linewidth for the main 1064 nm light becomes

$$L_{\text{FWHM,Main}} = 1.2 \text{ nm} \times \left( \frac{450}{\mathcal{F}} \right). \quad (2)$$

Here we normalized the cavity finesse by that of the arm cavity used in the Advanced LIGO detector. For the case of the Advanced LIGO arm cavity, the FWHM linewidth becomes 1.2 nm. For our tabletop setup, the FWHM linewidth becomes about 2.2 nm.

In order to evaluate the displacement noise of the ALS system, we used the main PDH signal as an out-of-loop sensor as shown in Fig. 1. Fig. 4 shows the measured displacement noise spectrum and its RMS. The right axis of this figure is the frequency noise,  $\delta\nu$ , which can be derived by

$$\frac{\delta\nu}{\nu} = \frac{\delta L}{L}, \quad (3)$$

where  $\nu$  is the laser frequency,  $\delta L$  is the cavity displacement noise, and  $L$  is the cavity length. The measured displacement RMS was about 0.7 nm at 0.1 Hz, which is below the FWHM linewidth of our cavity (2.2 nm). Therefore, the cavity displacement noise is successfully suppressed below its FWHM linewidth by the downconverted ALS system and even comparable to that of Advanced LIGO arm cavity FWHM linewidth.

The performance above  $\sim 1$  Hz is limited by an auxiliary PDH related noise, especially a sensor noise introduced by a commercially available broadband RFPD used for 2128 nm PDH lock. This can be improved by replacing the RFPD with custom resonant one which enhances the signal to noise ratio. Below  $\sim 1$  Hz, air turbulence through the intra-cavity beam is considered as the most dominant noise source. One possible coupling

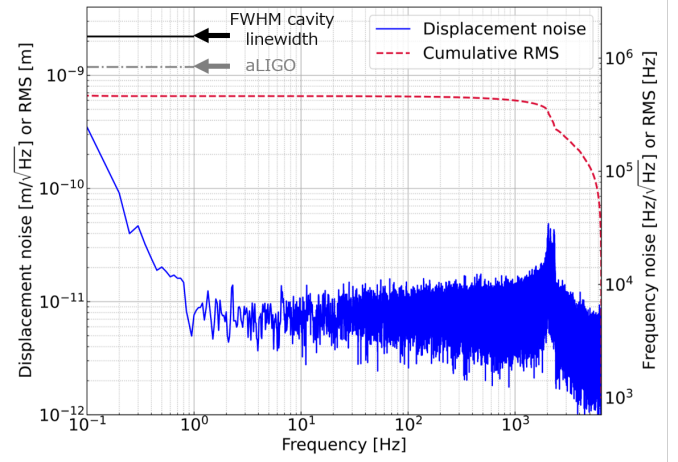


**Fig. 4.** Residual cavity displacement noise spectrum (blue solid line) and RMS (red dashed line). Black solid and grey dash-dotted lines are FWHM cavity linewidth of our setup and Advanced LIGO arm cavity, respectively. The relationship between the displacement noise (left axis) and the frequency noise (right axis) can be given by Eq. (3). The features around 2 kHz are due to the mechanical resonances of the cavity mirror mount.

mechanism is fluctuations of the refractive index of air which has the wavelength dependence [16]. Also, air turbulence can couple to the displacement noise through the beam jitter. The laser frequency noise is also one of the noise sources below  $\sim 1$  Hz.

From the results presented above, the main laser can be kept off resonance with cavity displacement noise less than its FWHM linewidth, and the main laser is no longer stochastically resonated in the cavity. By tuning the frequency offset between two lasers, the main laser can be brought to the resonance, and can hand over the PDH control. This means that the proof-of-concept of the ALS with downconverted 2128 nm light was demonstrated.

Here we discuss the scalability of this ALS system to a km-scale GWD. By replacing SHGs with OPOs, the frequency downconverted ALS can be installed to current GWDs. However, we need to carefully study the noise performance in terms of laser frequency to ensure proper operation [7]. As shown in Fig. 4, the measured noise with our setup was order of  $10^4$  Hz/ $\sqrt{\text{Hz}}$  in terms of frequency noise. One of the main noise sources is the auxiliary PDH related noise. This noise source scales with cavity length so that  $10^4$  reduction will be achievable since the arm cavity length of the Advanced LIGO detector is  $10^4$  times longer than our setup. Noise sources at low frequency region will be largely suppressed. Since the arm cavities are housed inside the vacuum chamber, noise induced by the air turbulence is not a limiting noise source [7]. The laser frequency is stabilized by mode-cleaning cavities and the auxiliary laser is tightly locked to the pre-stabilized main laser via phase-locked loop (PLL) [17]. This configuration results in the laser frequency noise well below the required level [7, 8]. The most important noise source, which does not scale to the arm cavity length and its suppression is nontrivial, is the intrinsic frequency noise of the OPO. In order to implement this ALS system to the upgraded GWDs, the bound on the frequency noise induced by the OPO needs to be investigated as the previous work that studied the

frequency noise introduced by an SHG [18].

As a future work, we are planning to install another OPO cavity and investigate the intrinsic OPO frequency noise. Moreover, the main dichroic cavity will be moved into a vacuum chamber with longer cavity length ( $\gtrsim 1$  m) and higher 1064 nm intra-cavity power. That setup will serve as a test bed to demonstrate a dichroic AlGaAs mirror and enable us to study the properties of such coatings under high beam intensity by combining with a phase camera [19]. Such dichroic AlGaAs mirrors require optimized layers to reduce thermo-optic noise [20]. Development of the optimized dichroic AlGaAs mirrors is ongoing and results will be presented in the future.

It should be mentioned that one of the advantages of using 2128 nm light is the ability to separate the two auxiliary beams of the x and y arm cavities. The Advanced LIGO ALS system distinguishes two green lights from two arm cavities by the beamsplitter, input test mass, and compensation plate wedges [4, 7]. This is enabled by the index of refraction difference in fused silica between 532 nm and 1064 nm lights;  $n = 1.46$  and  $1.45$  at  $\lambda = 532$  nm and 1064 nm, respectively [21]. For the 2128 nm light, the refractive index of the fused silica is 1.44, and the refractive index difference from the main 1064 nm light is about the same as that for the 532 nm light. Such refractive index difference will permit a beam axis separation using simply the wedges.

The downconverted ALS scheme described in this letter is applicable not only to crystalline AlGaAs coatings, but also to amorphous coatings such as amorphous silicon [22]. Furthermore, this ALS system enables the optimization of coating structures that can reduce the coating thermal noise [23]. Current arm cavity mirrors need to be dichroic in order to provide high reflectivity for both 1064 nm main laser and 532 nm green auxiliary laser as shown in Fig. 2 in Ref. [6]. The ALS presented in this letter introduces another degree of freedom to this dichroic mirror, i.e., high reflectivity at either 532 nm or 2128 nm.

As a summary, we have demonstrated a novel ALS system which allows the use of crystalline AlGaAs coated test masses, leading to improved detector sensitivity. The ALS scheme presented in this letter will help pave a path for improving the sensitivity of future upgraded GWs.

**Funding.** This work was supported with funding from the National Science Foundation grant PHY-2207640.

**Acknowledgments.** The authors thank Peter Fritschel, Yutaro Enomoto, and the LIGO Scientific Collaboration Optics Working Group for useful discussions and feedback. This paper has LIGO Document number LIGO-P2400168.

**Disclosures.** The authors declare no conflicts of interest.

**Data availability.** Data underlying the results presented in this paper are not publicly available at this time but may be obtained from the authors upon reasonable request.

## REFERENCES

1. B. P. Abbott *et al.*, Phys. Rev. Lett. **116**, 061102 (2016).
2. B. P. Abbott *et al.*, Phys. Rev. Lett. **119**, 161101 (2017).
3. R. Abbott *et al.*, Phys. Rev. D **103**, 122002 (2021).
4. J. Aasi *et al.*, Class. Quantum Gravity **32**, 074001 (2015).
5. A. J. Mullaev, B. J. J. Slagmolen, J. Miller, *et al.*, Opt. Express **20**, 81 (2012).
6. K. Izumi, K. Arai, B. Barr, *et al.*, J. Opt. Soc. Am. A **29**, 2092 (2012).
7. A. Staley *et al.*, Class. Quantum Gravity **31**, 245010 (2014).
8. T. Akutsu *et al.*, Class. Quantum Gravity **37**, 035004 (2020).
9. S. Gras and M. Evans, Phys. Rev. D **98**, 122001 (2018).
10. A. Buikema *et al.*, Phys. Rev. D **102**, 062003 (2020).
11. LIGO Scientific Collaboration, "LSC Instrument Science White Paper," <https://dcc.ligo.org/LIGO-T2300411/public> (2023).
12. G. D. Cole, S. W. Ballmer, G. Billingsley, *et al.*, Appl. Phys. Lett. **122**, 110502 (2023).
13. S. Adachi, J. Appl. Phys. **58**, R1 (1985).
14. R. W. P. Drever, J. L. Hall, F. V. Kowalski, *et al.*, Appl. Phys. B: Lasers Opt. **31**, 97 (1983).
15. C. Darsow-Fromm, M. Schröder, J. Gurs, *et al.*, Opt. Lett. **45**, 6194 (2020).
16. T. B. Quoc, M. Ishige, Y. Ohkubo, and M. Aketagawa, Meas. Sci. Technol. **20**, 125302 (2009).
17. D. Wolaver, *Phase-locked Loop Circuit Design*, Prentice Hall advanced reference series (Prentice Hall, 1991).
18. D. Yeaton-Massey and R. X. Adhikari, Opt. Express **20**, 21019 (2012).
19. E. Muñoz, V. Srivastava, S. Vidyant, and S. W. Ballmer, Phys. Rev. D **104**, 042002 (2021).
20. T. Chalermsongsak, E. D. Hall, G. D. Cole, *et al.*, Metrologia **53**, 860 (2016).
21. I. H. Malitson, J. Opt. Soc. Am. **55**, 1205 (1965).
22. J. Steinlechner and I. W. Martin, Phys. Rev. D **103**, 042001 (2021).
23. G. Venugopalan, F. Salces-Cárcoba, K. Arai, and R. X. Adhikari, Opt. Express **32**, 11751 (2024).